Biophysical Journal

Supporting Material

Mitoenergetic Dysfunction Triggers a Rapid Compensatory Increase in Steady-State Glucose Flux

Dania C. Liemburg-Apers,[1,3,4] Tom J. J. Schirris,[2,3] Frans G. M. Russel,[2,3] Peter H. G. M. Willems,[1,3,4] and Werner J. H. Koopman[1,3,4,*]

[1]Department of Biochemistry and [2]Department of Pharmacology and Toxicology, Radboud Institute for Molecular Life Sciences, Radboud University Medical Center, Nijmegen, The Netherlands; [3]Centre for Systems Biology and Bioenergetics, Radboud University and Radboud University Medical Center, Nijmegen, The Netherlands; and [4]Nijmegen Center for Mitochondrial Disorders, Radboud University Medical Center, Nijmegen, The Netherlands

APPENDIX A: SUPPLEMENTARY MATERIALS AND METHODS

Q-PCR analysis - RNA was extracted from C2C12 cells according to the manufacturer's protocol (**PureLink™ RNA Mini Kit, Invitrogen**). cDNA was generated from 1 µg RNA using the IScript cDNA synthesis kit (**Biorad, Hercules, CA, USA**) according to the manufacturer's protocol. Quantitative real-time PCR was performed in a final volume of 25 µl containing 12.5 µl SYBR®Green Supermix (**Bio-Rad**), 5 µl (10x diluted) cDNA, 4.5 µl RNAse-free water, 1.5 µl forward primer (2.5 µM) and 1.5 µl reverse primer (2.5 µM). Primers for GAPDH and Glut1-4 were obtained from **Biolegio, Nijmegen, The Netherlands (see table below)**. Amplification of cDNA was performed using a C1000 Thermal Cycler (**Bio-Rad**) and fluorescence was analyzed using the CFX96™ Real-Time System (**Bio-Rad**). The PCR conditions were 95º C for 3 minutes (1 cycle), 95º C for 15 s and 60º C for 30 seconds (39 cycles), and finally a temperature increase starting at 65º C to 95º C with 0.5º C intervals. RNA expression (N=3) was normalized against the mRNA level of GAPDH (DCt) and represented as $2^{-DC(t)}$ (**Fig. S1**).

Primer	Direction	Sequence
Glut1_mo_cDNA-F1	Forward (5'→3')	TGCAGTTCGGCTATAACACTG
Glut1_mo_cDNA-R1	Reverse (5'→ 3')	GGTGGTTCCATGTTTGATTG
Glut2_mo_cDNA-F1	Forward (5'→3')	TGTGATCAATGCACCTCAAG
Glut2_mo_cDNA-R1	Reverse (5'→ 3')	TCATAGTTAATGGCAGCTTTCC
Glut3_mo_cDNA-F1	Forward (5'→3')	ACTCTTTGTCAACCGCTTTG
Glut3_mo_cDNA-R1	Reverse (5'→ 3')	ATCTTGGCGAATCCCATAAG
Glut4_mo_cDNA-F1	Forward (5'→3')	CTTGGCTCCCTTCAGTTTG
Glut4_mo_cDNA-R1	Reverse (5'→ 3')	CACGTTGCATTGTAGCTCTG
GAPDH-F1	Forward (5'→3')	TGATGGGTGTGAACCACGAG
GAPDH-R1	Reverse (5'→ 3')	GGGCCATCCACAGTCTTCTG

Single cell pH measurements – For cytosolic pH analysis, C2C12 myoblasts were loaded with the pH-sensitive reporter molecule BCECF (2',7'-Bis-(2-carboxyethyl)-5-(and-6)-carboxyfluorescein) (Life Technologies - Molecular Probes**, Bleiswijk, The Netherlands**) by incubating them with 5 µM of the BCECF acetoxy-methyl (AM) ester form (BCECF-AM) in HT buffer for 15 min at 37º C in the dark. Subsequently, cells were washed 3 times with HT buffer and imaged using an inverted microscope (see above). The H^+-bound form of BCECF was excited at 440 nm (100 ms) using a 505DRLPXR dichroic mirror (XF2031; **Omega**). The H^+-unbound form of BCECF was excited at 490 nm (100 ms) using the same dichroic mirror. Fluorescence images were recorded at 530 nm using a 535AF45 emission filter (XF3084; **Omega**). The ratio between the emission signal obtained at 490 and at 440 excitation was used as a measure of cellular pH (**1**). Time-lapse recordings were performed using an acquisition interval of 6 s. (**Fig. S2C-D**)

P/O ratio analysis - To determine the P/O ratio we slightly modified a previously described approach (**2**). Briefly, cells were resuspended in mitochondrial respiration medium MiR05 (**3**) containing: 110 mM sucrose, 60 mM K^+-lactobionate, 0.5 mM EGTA, 3 mM $MgCl_2$, 20 mM taurine, 10 mM KH_2PO_4, 20 mM HEPES adjusted to pH 7.1 with KOH at 30 °C, and 1 g/l BSA essentially fatty acid-free. Routine O_2 consumption was recorded as described in the Materials and Methods section. Next, the plasma membrane was permeabilized using digitonin (10 µg /

$1 \cdot 10^6$ cells) and malate (MAL, 2 mM) and pyruvate (PYR, 5 mM) were added (**Fig. S6**). Upon addition of ADP (220 nM), the O_2 consumption rate was allowed to decrease to a stable level, indicating a complete conversion of ADP into ATP. As a quality control (**4**), mitochondrial integrity was assessed by adding 10 µM cytochrome-*c* (cyt-*c*). The P/O ratio was calculated by dividing the amount of ADP used by the amount of oxygen used by the mitochondria to consume all the ADP.

APPENDIX B: SUPPLEMENTARY RESULTS

B1. Validation of the glucose uptake and consumption measurements - Various control experiments were performed to validate the strategy proposed in the previous section. To block Glut-mediated GLC uptake we used the inhibitor CytoB. Indeed, C2C12 cells pretreated with CytoB did not show an increase in $[GLC]_c$ upon extracellular GLC application (**Fig. S2A**). However, CytoB might also induce F-actin depolymerization at the same concentration that inhibits cellular GLC uptake (**5**). To investigate whether this off-target effect was responsible for the blocking of GLC entry we carried out experiments with the CytoB structural analogue Cytochalasin D (CytoD). This compound is an established inhibitor of actin polymerization (**6**) but does not affect Gluts (**7**). In contrast to CytoB, GLC entry was not blocked by CytoD in IAA-treated cells (**Fig. S2A**). This strongly suggests that the GLC influx blocked by CytoB is Glut-mediated. Proteinaceous FRET sensors can exhibit sensitivity to their local environment including pH (**8-10**). C2C12 cells transfected with a high-affinity GLC sensor (FLIPglu-170nδ13V; K_m= 0.17 µM; (**11**) did not display changes in fluorescence ratio signal upon manipulation of the extracellular GLC level (**Fig. S2B**). This suggests that this cytosolic sensor is fully in its GLC-bound state ("saturated") and that the observed changes in FLII ratio are unlikely caused by GLC-independent alterations in FRET efficiency. Moreover, in agreement with the data presented in **Fig. 1B** (upper panel), the lack of effect on the high-affinity GLC sensor fluorescence signals, directly after GLC addition, demonstrates that $[GLC]_{ext}$ changes do not induce cell-volume changes. Cytosolic pH was not significantly affected by IAA treatment (500 µM for 15 min; **Fig. S2C**). However, inhibition of oxidative phosphorylation using piericidin A (PA) or antimycin (AA; see below) induced cytosolic acidification (**Fig. S2C**). Therefore we determined whether pH changes affected the fluorescence ratio signal of FLII by transient addition of extracellular ammonium chloride (**1**). Using the pH-sensor BCECF we observed that NH_4Cl addition and removal induced cytosolic alkalinization and acidification, respectively (**Fig. S2D**; upper panel). However, no changes in the FLII ratio signal were observed upon acidification (**Fig. S2D**; lower panel). These results, combined with the observation that CFP and $Citrine_{FRET}$ emission changed antiparallel (**Fig. 1B**), make it unlikely that FLII signals were affected by cytosolic acidification in our experiments.

B2. FLII calibration simulation -Simulating the calibration procedure with the optimal model (vehicle-condition) predicted that $[GLC]_c$ fully equilibrated with $[GLC]_{ext}$ within 30 min for $[GLC]_{ext} \leq 4$ mM (**Fig. S4A**). For $[GLC]_{ext} > 4$ mM this model predicted that $[GLC]_c$ did not fully equilibrate with $[GLC]_{ext}$ within this time period (**Fig. S4A**). However, correcting $[GLC]_c$ for this effect did not significantly affect the FLII calibration curve and its K_m and R_{max} value (**Fig. S4B**).

APPENDIX C: SUPPLEMENTARY FIGURES

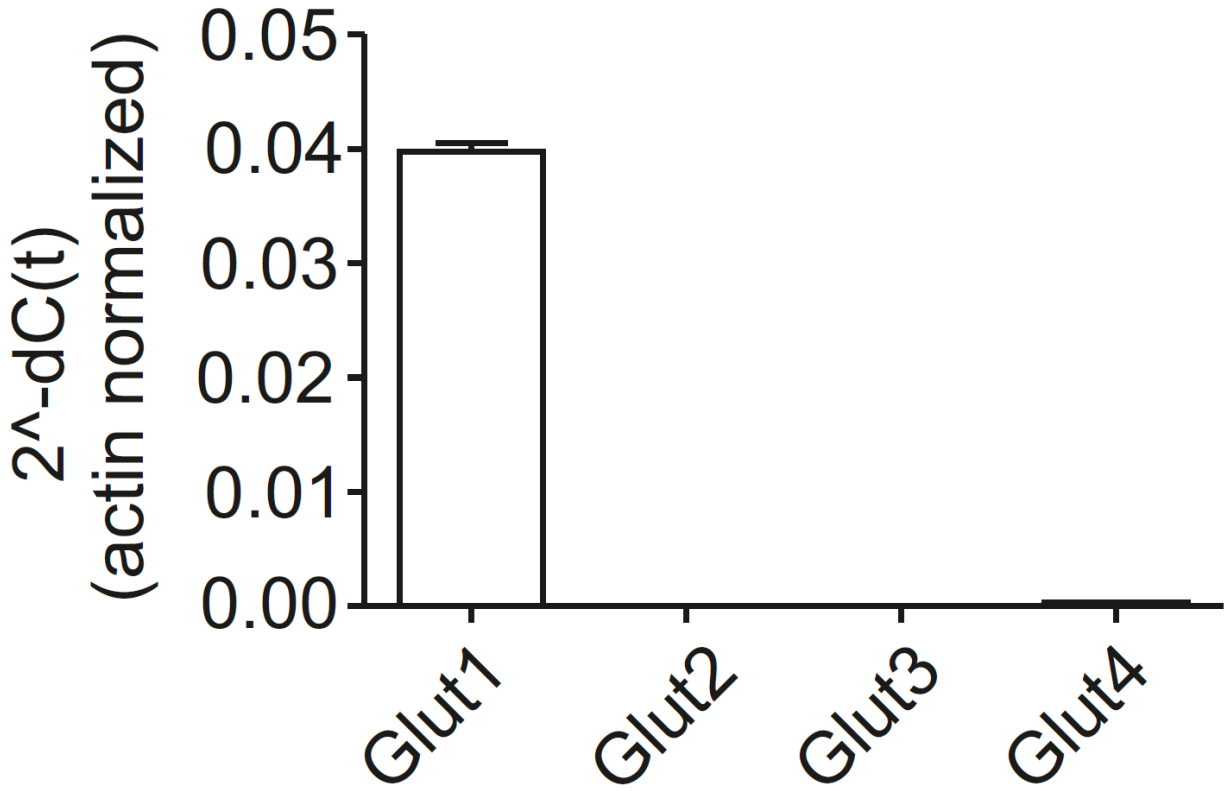

Figure S1. mRNA levels of Glut family members in C2C12 myoblasts and respirometry analysis. *A qPCR with primers against mouse Glut1, Glut2, Glut3, and Glut4 was performed on cDNA generated from C2C12 myoblasts. Only mRNA of Glut1 was detected.*

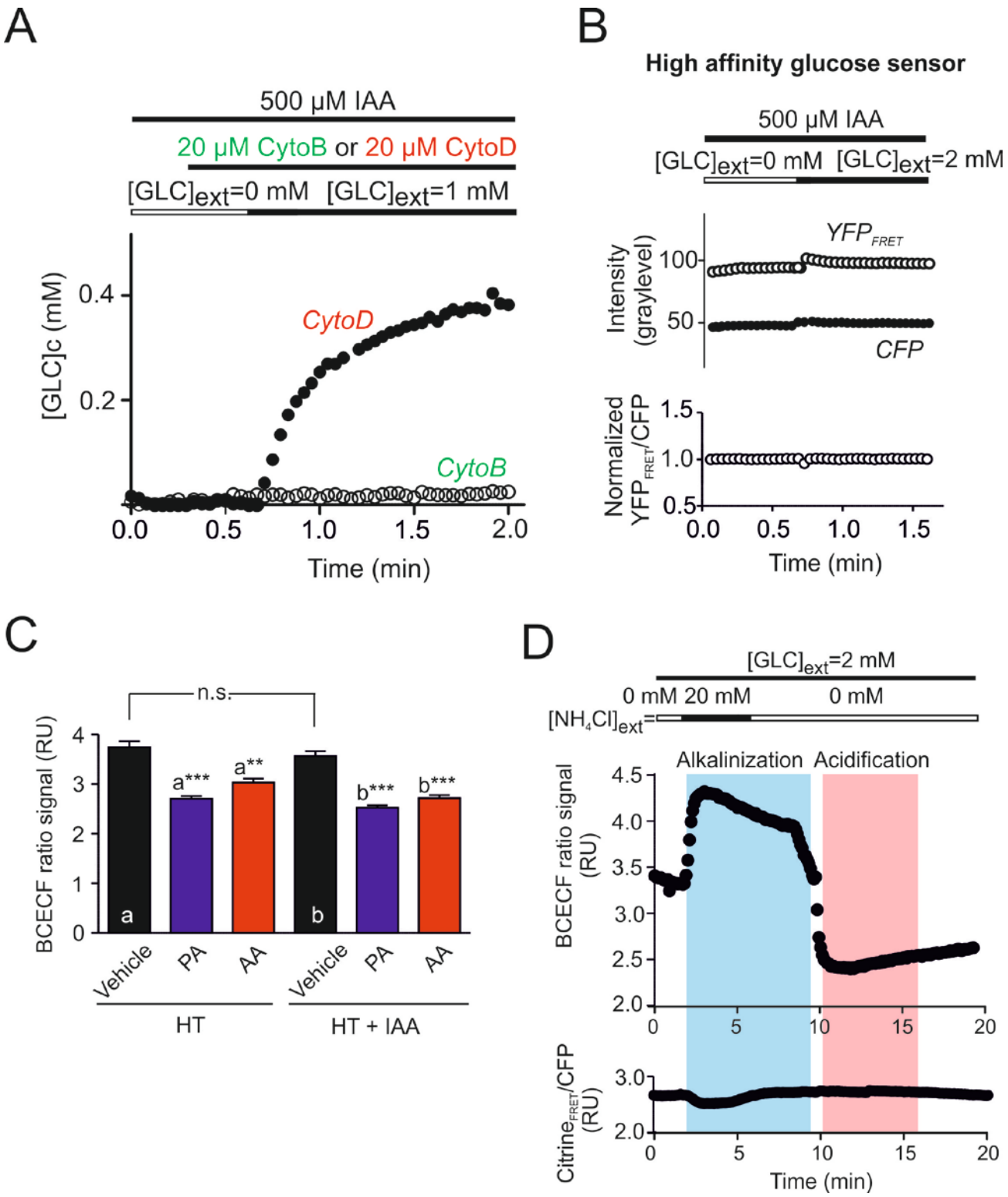

Figure S2. Validation of the experimental strategy for analysis of glucose uptake and consumption. (**A**) Typical GLC uptake in cells pretreated with CytoB (open symbols) or CytoD (filled symbols). (**B**) Typical GLC uptake in cells expressing a high-affinity GLC sensor (FLIPglu-170nδ13V). (**C**) Effect of the various treatments on cytosolic pH. Cells were pretreated for 30 min with vehicle, PA or AA. Subsequently, cells were loaded with the pH sensor BCECF using a $[GLC]_{ext}$ of 0 mM in the absence or presence of IAA. Statistical significance was determined using the Kruskal-Wallis test: N.s. not significant. (**D**) Effect of cytosolic pH changes on FLII fluorescence. Cytosolic pH was manipulated by transient extracellular addition ammonium chloride and monitored using the pH sensor BCECF (upper panel). In parallel experiments the response of FLII to these changes was determined (lower panel).

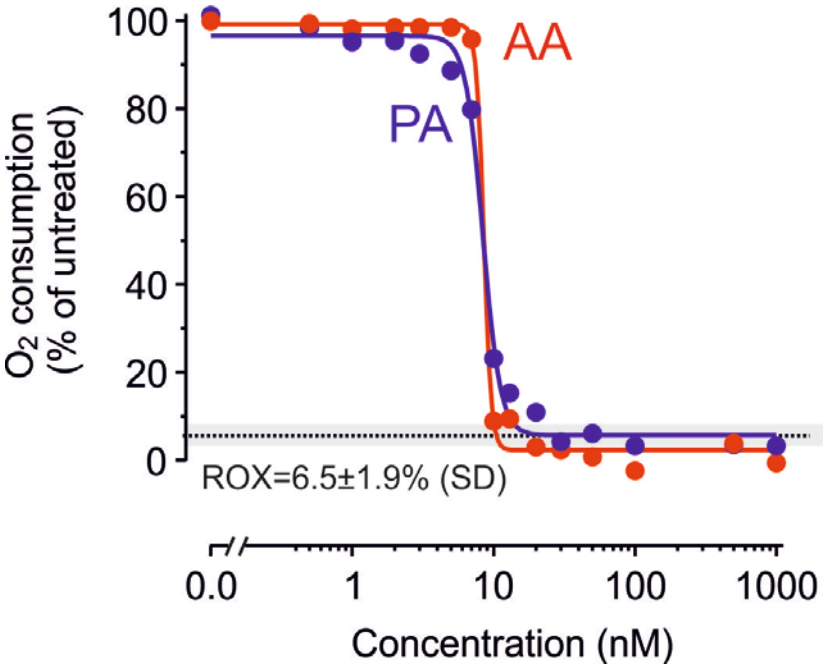

Figure S3. Dose-dependent inhibition of O_2 consumption by piericidin A and antimycin A in intact C2C12 cells. O_2 consumption rates of C2C12 cells in culture medium upon titration with piericidin A (PA) and antimycin A (AA). Respiration rates were normalized to basal respiration in the absence of inhibitor. The IC_{50} value was determined by fitting a logistic equation ($y=[(A_1-A_2)/(1+(x/IC_{50})^p)]-A_2$ to the data ($R^2>0.95$), with A_1 being the initial respiration (*i.e.* 100%) and A_2 being the lowest respiration. Residual respiration (ROX) after rotenone (ROT) and antimycin A (AA) was displayed as percentage of basal respiration.

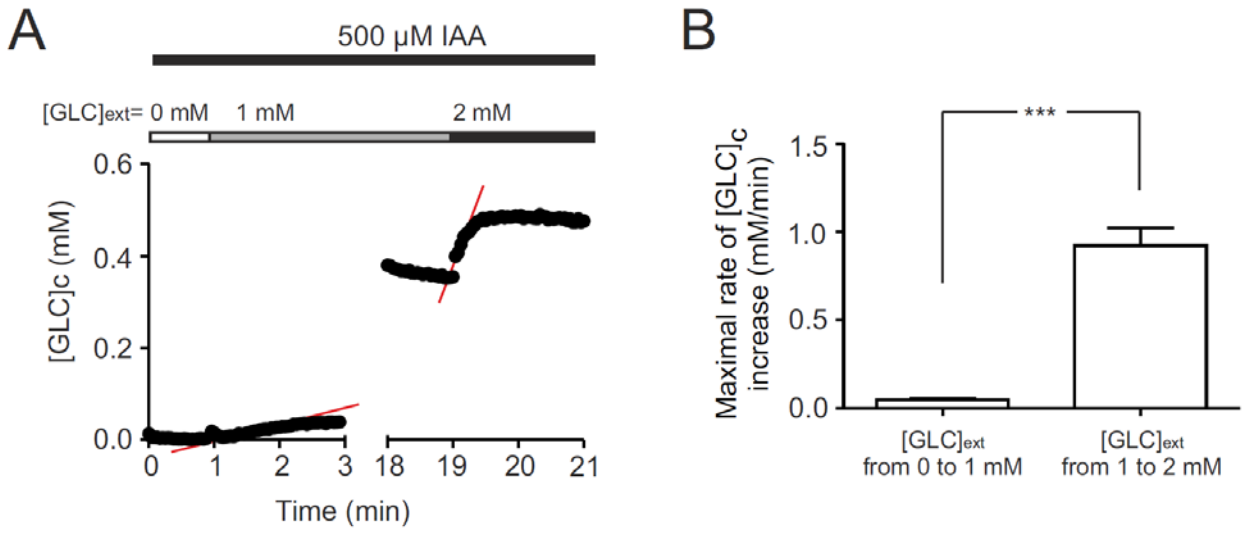

Figure S4. Effect of $[GLC]_c$ on the maximal rate of $[GLC]_c$ increase. (**A**) Typical kinetics of $[GLC]_c$ upon acutely increasing $[GLC]_{ext}$ from 0 to 1 mM (left part) and from 1 mM to 2 mM (after a 15 min waiting period; break). The experiment was carried out in the presence of IAA to block GLC consumption. The maximal rate of $[GLC]_c$ increase was quantified using a linear fit (red lines). (**B**) Average maximal rate of $[GLC]_c$ increase for the experiment depicted in panel A (N=2 experiments, n=18 cells).

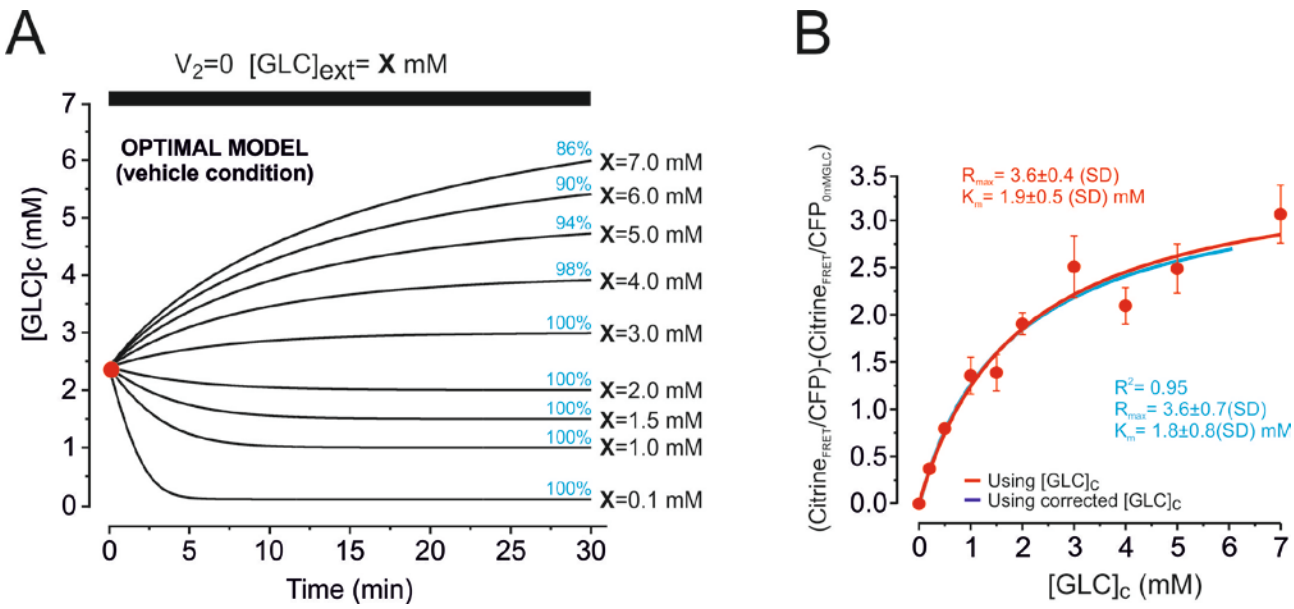

Figure S5. Effect of the magnitude of $[GLC]_{ext}$ on $[GLC]_c$ equilibration kinetics as predicted by the optimal model. (A) Simulations with the vehicle model were carried out to reflect the conditions during the FLII calibration protocol: At $t=t_0$ $[GLC]_{ext}$ increases to values (**X**) used during calibration (see **Fig. 1C**); the simulation time is 30 min to reflect the incubation time. **Initial conditions:** $[GLC]_{ext}$=25 mM, $[GLC]_c$=2.4 mM, V_2=0 to reflect the presence of IAA. After 30 min, full equilibration is predicted (*i.e.* $[GLC]_{ext}=[GLC]_c$) for **X**=0.1 mM, 1.0 mM, 1.5 mM, 2.0 mM, 3.0 mM and 4.0 mM. Partial equilibration was predicted for **X**=5.0 mM ($[GLC]_c$ equals 94% of $[GLC]_{ext}$), **X**=6.0 mM ($[GLC]_c$ equals 90% of $[GLC]_{ext}$) and **X**=7.0 mM ($[GLC]_c$ equals 86% of $[GLC]_{ext}$). The predicted partial equilibration at higher $[GLC]_{ext}$ did not affect the FLII calibration curve, since identical values for R^2, R_{max} and K_m were obtained (panel **B**).

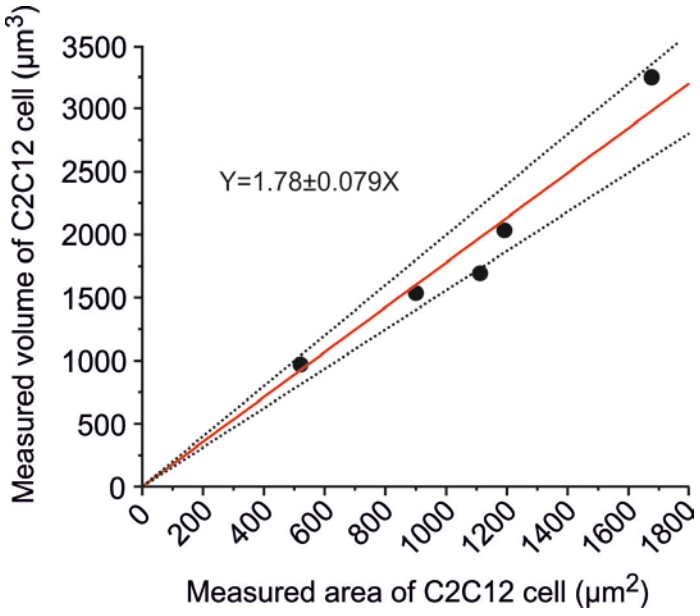

Figure S6. Area-volume relationship of C2C12 cells. To calculate the relationship between C2C12 cell area and volume we used data from 3D morphometric measurements of C2C12 cell (**12**). The relationship between area and volume was fitted using a linear equation (slope=1.78±0.08, p=0.001, R^2=0.98). Dotted lines indicate 95% confidence limits.

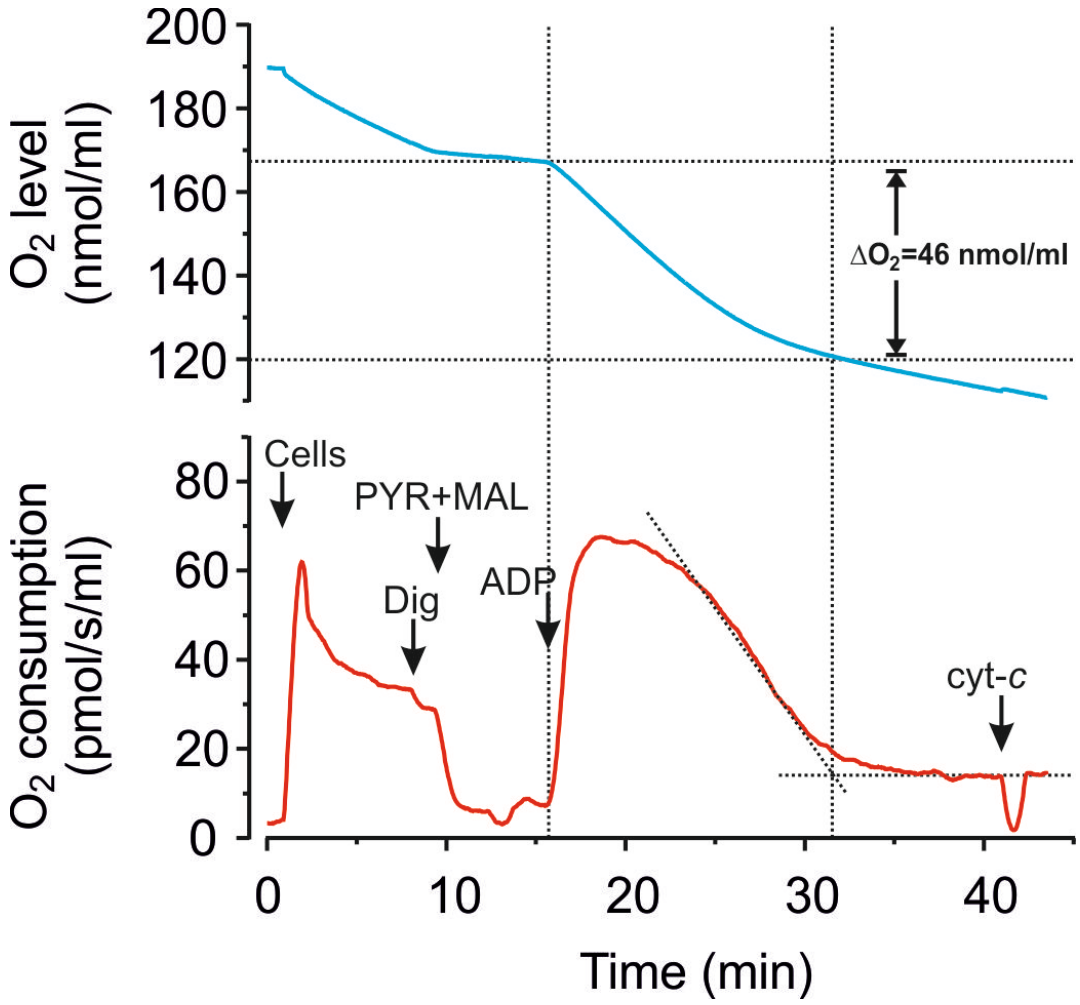

Figure S7. Quantification of P/O ratio in permeabilized C2C12 cells. C2C12 cells were added to the respirometry chamber and permeabilized using the detergent digitonin (Dig). Subsequently, pyruvate/malate (PYR+MAL) and ADP (220 nM) were added. The total amount of O_2 consumed (ΔO_2) following ADP addition allowed calculation of the P/O ratio. Mitochondrial integrity was assessed by adding cytochrome-*c* (cyt-*c*). This figure depicts a representative example of 4 independent experiments.

APPENDIX D: SUPPLEMENTARY REFERENCES

1. Ozkan, P., and R. Mutharasan. 2002. A rapid method for measuring intracellular pH using BCECF-AM. Biochim Biophys Acta 1572:143-148.
2. De Rasmo, D., G. Gattoni, F. Papa, A. Santeramo, C. Pacelli, T. Cocco, L. Micelli, N. Sardaro, M. Larizza, M. Scivetti, S. Milano, and A. Signorile. 2011. The beta-adrenoceptor agonist isoproterenol promotes the activity of respiratory chain complex I and lowers cellular reactive oxygen species in fibroblasts and heart myoblasts. Eur J Pharmacol 652:15-22.
3. Krumschnabel, G., M. Fontana-Ayoub, Z. Sumbalova, J. Heidler, K. Gauper, M. Fasching, and E. Gnaiger. 2015. Simultaneous high-resolution measurement of mitochondrial respiration and hydrogen peroxide production. Methods Mol Biol 1264:245-261.
4. Kuznetsov, A. V., V. Veksler, F. N. Gellerich, V. Saks, R. Margreiter, and W. S. Kunz. 2008. Analysis of mitochondrial function in situ in permeabilized muscle fibers, tissues and cells. Nat Protoc 3:965-976.
5. Bonder, E. M., and M. S. Mooseker. 1986. Cytochalasin B slows but does not prevent monomer addition at the barbed end of the actin filament. J Cell Biol 102:282-288.
6. Casella, J. F., M. D. Flanagan, and S. Lin. 1981. Cytochalasin D inhibits actin polymerization and induces depolymerization of actin filaments formed during platelet shape change. Nature 293:302-305.
7. Carruthers, A. 1990. Facilitated diffusion of glucose. Physiol Rev 70:1135-1176.
8. Borst, J. W., M. A. Hink, A. van Hoek, and A. J. Visser. 2005. Effects of refractive index and viscosity on fluorescence and anisotropy decays of enhanced cyan and yellow fluorescent proteins. J Fluoresc 15:153-160.
9. Willemse, M., E. Janssen, F. de Lange, B. Wieringa, and J. Fransen. 2007. ATP and FRET--a cautionary note. Nat Biotechnol 25:170-172.
10. Moussa, R., A. Baierl, V. Steffen, T. Kubitzki, W. Wiechert, and M. Pohl. 2014. An evaluation of genetically encoded FRET-based biosensors for quantitative metabolite analyses in vivo. J Biotechnol 191:250-259.
11. Takanaga, H., and W. B. Frommer. 2010. Facilitative plasma membrane transporters function during ER transit. FASEB J 24:2849-2858.
12. Slomka, N., and A. Gefen. 2011. Cell-to-cell variability in deformations across compressed myoblasts. J Biomech Eng 133:081007.